Available online at www.sciencedirect.com
SCIENCE DIRECT®
Methods 37 (2005) 154–164
METHODS
www.elsevier.com/locate/ymeth

Photobleaching approaches to investigate diffusional mobility and trafficking of Ras in living cells

J. Shawn Goodwin, Anne K. Kenworthy *

Departments of Molecular Physiology & Biophysics and Cell & Developmental Biology, 718 Light Hall, Vanderbilt University School of Medicine, Nashville, TN, 37232, USA

Accepted 24 May 2005

Abstract

Recent advances in our understanding of the intracellular trafficking, membrane microenvironment, and subcellular sites of signaling of Ras have been driven by observations of GFP-tagged Ras in living cells. Here, we describe methods to gain further insight into the regulation of these events through the use of quantitative fluorescence microscopy. We focus on three techniques, fluorescence recovery after photobleaching (FRAP), fluorescence loss in photobleaching (FLIP), and selective photobleaching. While all of these techniques exploit photobleaching as a tool to monitor protein dynamics, they each provide a unique subset of information. In particular, FRAP provides measurements of protein mobility via lateral diffusion by monitoring recovery of fluorescence into a region following a single photobleaching event. FLIP assesses the level of continuity and communication between subcellular compartments by repetitively photobleaching a region of interest and following concomitant loss of fluorescence from other areas in the cell. Selective photobleaching reveals kinetic information about active and passive transport of proteins into organelles such as the Golgi complex or between areas of protein enrichment such as caveolae. We describe how to implement these techniques using commercially available confocal microscopes and outline methods for data analysis. Finally, we discuss how these approaches are being used to provide new insights into the mechanisms of membrane microdomain localization, vesicular versus non-vesicular transport, and kinetics of exchange of Ras on and off of cell membranes.

Keywords: Ras; GFP; Photobleaching; FRAP; Fluorescence microscopy; Lateral diffusion; Intracellular trafficking

1. Introduction

The use of GFP to fluorescently monitor proteins in living cells has become an important tool in cell biology [1]. Visualization of GFP-Ras has contributed tremendously to our understanding of Ras biology. Discoveries of the trafficking of newly synthesized Ras through the secretory pathway, compartmentalization of Ras isoforms in membrane microdomains at the cell surface, and signaling of Ras from intracellular compartments all have depended on imaging of GFP-Ras in combination with techniques such as biochemical fractionation and immunoelectron microscopy (reviewed in [2–5]). The high spatial and temporal resolution provided by live cell imaging techniques offers the potential for unique insights into the study of Ras biology. One example is the ability to monitor multiple subcellular pools of Ras simultaneously, an important capacity given recent findings that Ras resides in several intracellular compartments depending on its activation state, trafficking itinerary, or state of posttranslational processing [2,4,6–12].

Here, we discuss three live cell imaging techniques that can be used to monitor Ras dynamics within the cell: fluorescence recovery after photobleaching (FRAP), fluorescence loss in photobleaching (FLIP),

* Corresponding author. Fax: +1 615 322 7236.
E-mail address: anne.kenworthy@vanderbilt.edu (A.K. Kenworthy).

1046-2023/$ - see front matter © 2005 Elsevier Inc. All rights reserved.
doi:10.1016/j.ymeth.2005.05.013

and selective photobleaching. Each of these approaches utilizes a combination of time-lapse imaging and photobleaching in order to mark and subsequently follow the movement of a discrete pool of Ras within the cell. The photobleaching event renders the existing molecules in the chosen region dark, allowing for subsequent monitoring of the influx (by either active or passive processes) of fluorescent molecules into the area. With these approaches, Ras diffusion and trafficking can be qualitatively and quantitatively documented. While these photobleaching techniques have similarities in their implementation and interpretation, each provides unique information as well.

Below we discuss the principles underlying FRAP, FLIP, and selective photobleaching. We next provide detailed protocols for these experiments and finally discuss recent applications of these approaches to the study of Ras.

2. Principles of FRAP, FLIP, and selective photobleaching

For additional information on these techniques, see [1,13–19]. Related approaches that may be of interest but that are outside the scope of this article include fluorescence correlation spectroscopy [20], single molecule tracking [21], and photoactivatable GFP [22,23].

2.1. FRAP

FRAP is a technique that monitors diffusion of fluorescent molecules into a region in which fluorophores have been irreversibly photobleached by a high intensity laser pulse. Classic FRAP measurements monitored recovery into a diffraction-limited spot [13]. However, as we will discuss, through the use of confocal FRAP the geometry and size of the bleached region can be easily modified. From the data generated with this method, the effective diffusion coefficient (D) of a molecule can be estimated based on the half time ($t_{1/2}$) of recovery into the bleached region (Fig. 1). In addition, the recovery curve provides the percentage of mobile and immobile proteins (Fig. 1). The magnitude of D provides information about the state of the labeled protein (soluble versus membrane bound) as well as barriers to free diffusion, while the mobile fraction reports on the percentage of molecules that are free to diffuse over the time course of the experiment.

FRAP is not limited to measurements of lateral diffusion. Dynamic exchange with a cytoplasmic pool versus lateral diffusion can be detected by varying the size of the bleached region [12]. The rate of membrane exchange occurs independently of the size of the bleached area. For lateral diffusion, the ratio of the diffusion times should remain constant with varying bleach spot

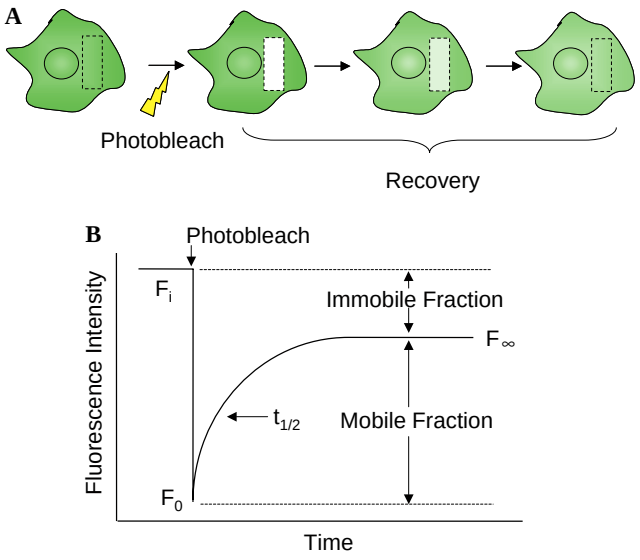

Fig. 1. Principle of confocal FRAP. (A) This technique is used to monitor the diffusive recovery of fluorescent proteins rendered dark (i.e., photobleached) by a high intensity laser pulse within a region of interest (box). Prebleach and postbleach images are acquired at low excitation intensity in order to minimize overall photobleaching during data collection. Both the size and geometry of the bleach region can be varied as desired in confocal FRAP. Note that when the bleach region is large, a loss of fluorescence outside the bleached region will occur as the result of dilution by the bleached molecules. (B) The recovery of fluorescent molecules into the bleached region yields a characteristic recovery curve. From this curve the $t_{1/2}$ (used to calculate D) and M_f can be determined. Alternatively, D can be calculated from the recovery images using a simulation that takes compartment geometry into account (see text for details).

sizes [12,24,25]. FRAP studies of Ras have utilized both traditional spot photobleaching approaches [12,24,25] and a confocal FRAP method [26] that we will describe in detail below.

2.2. FLIP

FLIP examines the continuity of compartments within a cell (Fig. 2). Here, the region of interest is subjected to multiple bleaches, allowing time in between for recovery of fluorescent material (by either diffusion or transport) back into the bleach area. This method reveals which areas of the cell outside of the photobleached region can contribute to the recovery of fluorescence, in effect defining compartmental boundaries. In addition, the rate of loss of fluorescence reflects the kinetics of trafficking or diffusion between the compartments or regions of the cell. FLIP can also reveal the structure of compartments that are not in dynamic equilibrium with the bleached region, as fluorescence in these compartments will remain unaltered [27,28]. This method has been used to examine proteins associated with the plasma membrane, endoplasmic reticulum (ER), Golgi complex, nucleus, and the cytoplasm [1,27–34].

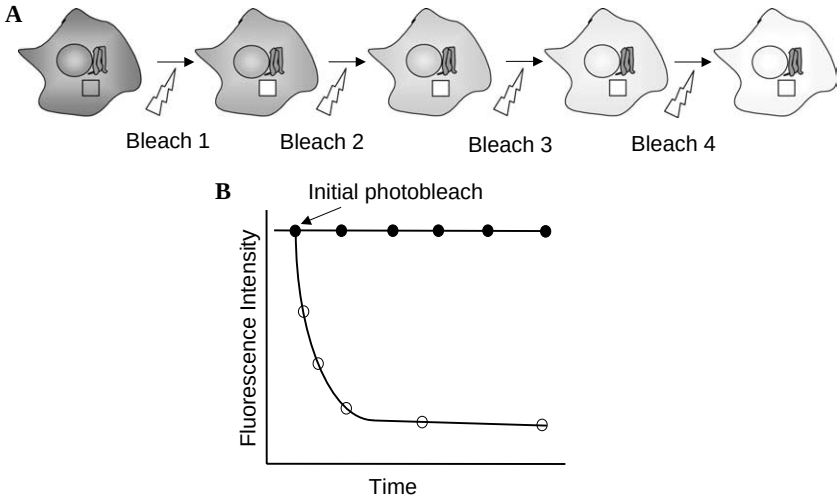

Fig. 2. Principle of FLIP. Repetitively photobleaching a region of the cell can determine the extent of continuity/communication with other compartments within the cell. (A) In this example, a hypothetical protein localized to both the Golgi complex and cell surface is shown. Repetitive bleaching of the plasma membrane (box) depletes cell surface fluorescence but not the Golgi pool. (B) Fluorescence is lost for proteins that are continuous with the bleached region (open circles). The rate of loss of fluorescence may vary depending on the extent and mechanism of communication between compartments. In contrast, no loss in fluorescence is observed for regions that are not in communication with the bleached region over the time course of the experiment (closed circles).

2.3. Selective photobleaching

This method is very similar to FRAP in principle, but allows for measurements of protein dynamics between compartments within the cell. Recoveries here can occur via diffusion, exchange on and off a membrane, or vesicular transport. In combination with time-lapse imaging, specific regions of interest, often organelles such as the Golgi complex [34,35] or areas of protein localization such as caveolae [28] are photobleached, and the recovery of fluorescently tagged molecules into the bleached region is monitored (Fig. 3). Therefore, selective photobleaching extends the usefulness of the traditional FRAP technique by monitoring kinetics of recovery for discrete structures. It can also be used to enhance the fluorescence of dim objects. For example, the biosynthetic trafficking of proteins in Golgi-derived transport carriers to the plasma membrane is more easily visualized when the fluorescence of the preexisting plasma membrane pool is eliminated by photobleaching [34].

3. Methods

3.1. Sample preparation

3.1.1. DNA constructs

Due to the C-terminal processing of Ras, N-terminally tagged GFP-Ras constructs are used. Here, the Ras DNA sequence is ligated into an enhanced GFP (GFP) vector downstream of the coding information for the fluorescent protein as described in Choy et al. [10]. Similar Ras constructs have been described by a number of groups, and importantly, attachment of GFP does not appear to interfere with Ras function [9–11,36–40]. YFP can also be used for photobleaching applications; however, YFP is less photostable than GFP, and therefore more photobleaching may occur during time-lapse imaging. CFP-tagged proteins are avoided due to the toxicity of CFP on the cell after photobleaching.

3.1.2. Cell culture and transfections

COS-7 cells are used in the experiments described below, because they are readily transfected and have large, flat plasma membranes that make them amenable for FRAP measurements. Cells are cultured using standard procedures as previously described [26,34,41]. Briefly, cells are grown at 37 °C and 5% CO_2 in standard tissue culture flasks in DMEM supplemented with 10% fetal calf serum. For live cell imaging, cells are seeded onto glass coverslips (12 mm circle, number 1.5) in a 6-well plate, typically 3–4 coverslips per well, and grown using the conditions described above. After 1 day of growth, cells are transfected with DNA using FuGENE 6 (Roche Diagnostic, Indianapolis, IN) transfection reagent as per the protocol provided by the manufacturer (normally 1 μg of DNA per well in a 6-well plate). Other cell lines may require different reagents or methods to provide the most efficient transfections. One day after transfection, cells are imaged as described below. Cells can alternatively be grown in Lab-Tek chambered coverglasses or other dishes for live cell imaging.

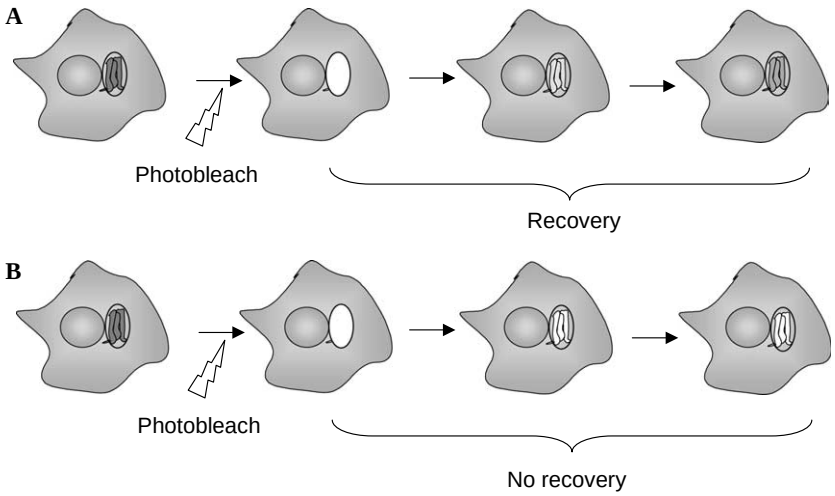

Fig. 3. Principle of selective photobleaching. Like FRAP, selective photobleaching utilizes a single bleach event to render a population of fluorescent proteins dark. In this case, however, the bleached region is typically an organelle or transport intermediate, allowing for visualization of movement of proteins between subcellular compartments. Here, a hypothetical protein localized to the plasma membrane and Golgi complex is shown. In order to determine if the protein can traffic from the plasma membrane to the Golgi complex, selective photobleaching is used to deplete the fluorescence from the Golgi-associated molecules. Because the bleaching is not confined to a single focal plane, a minor amount of the cell surface pool is lost upon bleaching of molecules in the Golgi complex. (A) Recovery of the Golgi-associated pool over time provides evidence for trafficking of the protein from the plasma membrane to the Golgi complex. Of course, to confirm that this protein is derived from the cell surface, alternative sources of fluorescence recovery such as newly synthesized proteins also need to be ruled out. (B) Lack of recovery of the Golgi pool indicates that retrograde transport from the cell surface to the Golgi does not occur over the time course of the experiment.

3.1.3. Live cell imaging

Cells grown on coverslips are mounted on a chamber containing imaging buffer either with or without serum depending on the experimental conditions being tested. Cells are imaged in buffer consisting of DMEM, 10% fetal calf serum, and 25 mM Hepes buffer. Coverslips are inverted onto a chamber created by punching a hole in a silicon gasket, mounted onto a glass slide with petroleum jelly or silicon grease. For imaging at 37 °C, the stage temperature is controlled by a Nevtek Air Stream Stage Incubator (Burnsville, VA); however, any appropriate stage heater may be used.

3.2. Instrumentation

These techniques require a confocal microscope with the capability of imaging GFP and performing time-lapse imaging in conjunction with bleaching subroutines. For our investigation, a Zeiss LSM 510 confocal (Carl Zeiss, Thornwood, NY) equipped with physiology software was utilized. The software on this instrument allows the user to set the acquisition time and number of images collected, define a region of interest in which the sample will be photobleached, and rapidly modulate laser transmission between bleaching and monitoring conditions. This setup allows for rapid data collection and observation of protein recovery into the bleached region. However, consideration must be given to balancing the sampling frequency and obtaining images with low noise and high dynamic range [17]. For protocols utilizing FRAP and FLIP on a Zeiss 410 LSM confocal microscope (and equivalent instruments) see [32]. A dedicated FRAP machine can alternatively be used for diffusional measurements, as described elsewhere [13]. In the protocols outlined below, we assume that the operator is familiar with the basic operation of the confocal microscope and focus mainly on details specific to the photobleaching experiments.

3.3. Confocal FRAP

3.3.1. Establish conditions for FRAP measurements

(1) *Define the imaging conditions for monitoring fluorescence recovery.* Determine the appropriate filter sets, objective, zoom, scan speed, pinhole settings, excitation intensity, detector gain, and line averaging to obtain images with high signal but a minimum of saturated pixels. Our experiments typically utilize a Plan-Neofluar 40×1.3 numerical aperture (NA) oil DIC or PlanApochromat 100×1.4 NA oil DIC lens at a zoom of 4× and 2×, respectively. GFP is excited with the 488 nm line of a 40 mW argon laser at 60% power and 0.1–1% transmission and fluorescence emission collected using a 505 long pass filter. The pinhole is set at 1 Airy unit and no line averaging is used. It is particularly important to set the laser transmission to a level that will not cause bleaching of the sample during monitoring of fluorescence recovery, yet will give good image resolution. To determine if overall bleaching is occurring at the attenuated laser level, execute a time series measurement without a high intensity bleaching laser pulse.

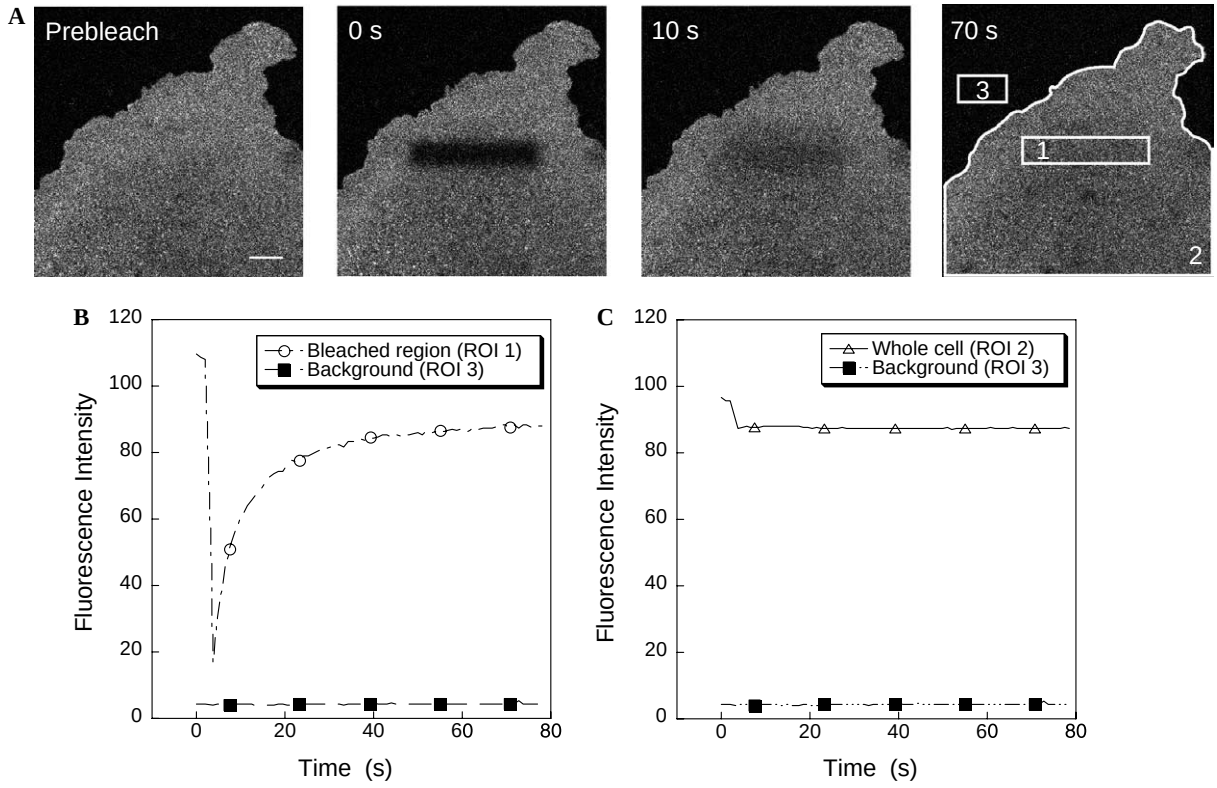

Fig. 4. Example of a confocal FRAP experiment. (A) Selected images from a confocal FRAP experiment on GFP-NRas expressed in COS-7 cells. The first image obtained after photobleaching is designated as $t = 0$ s. Examples of ROIs defined to monitor the fluorescence are shown in the final panel. These include (1) the bleached region, (2) the "whole cell," and (3) a background region. Bar, 5 μm. (B) Example of raw data for the bleached region for a typical confocal FRAP experiment. Note the smooth rise in fluorescence intensity, which plateaus at long times. For clarity, individual data points are not shown. (C) Example of raw data for whole cell fluorescence. Following a drop in fluorescence corresponding to the loss of fluorescent material due to the photobleaching event, the intensity remains constant. This indicates no drifting of the focal plane or photobleaching at the attenuated laser level have occurred during the recovery portion of the experiment.

(2) *Choose the bleach region.* The choice of the bleach region is governed by the size of the cells, the speed of fluorescence recovery, and the desired method of analysis. Typically, we define a rectangle, which is 4 μm wide (Fig. 4A). In this region, GFP-Ras generally fully recovers in ~70 s at 25 °C, with a mobile fraction (M_f) of ⩾90% (Fig. 4B). However, other bleach geometries or sizes can be used as needed. Recoveries will occur more quickly for smaller bleach regions (Fig. 5). For ease of analysis, we suggest that the bleached region coordinates remain constant between measurements. The image can be adjusted to place the bleach region to the desired location of the cell.

(3) *Determine conditions for bleaching.* Using a fixed sample, determine the number of high intensity (100% transmission) bleach iterations that will be needed to irreversibly photobleach the fluorescent protein in the bleach region to background levels. A single laser pulse will in most cases not be sufficient to completely bleach all of the molecules in the region of interest. We have found that 10 bleach iterations at 100% transmission of a 40 mW argon laser are sufficient to bleach GFP using a 40× 1.4 NA objective at 4× digital zoom.

(4) *Choose the region in which to monitor fluorescence recovery.* Depending on the method chosen for data analysis, it is not always necessary to monitor fluorescence recoveries by collecting images of the whole cell (or a large region of the cell). Instead, data can be collected only for the bleach region of interest (ROI). This approach greatly speeds data acquisition. However, it sacrifices information about overall photobleaching and/or focal plane drifts that can be readily assessed by examination of changes in fluorescence that occur in the area surrounding the bleach (Fig. 6).

(5) *Establish the time required for full fluorescence recovery.* Determine the appropriate length of time needed for recovery of bleached molecules to plateau. Set the total number of images to collect based on the time fluorescence recovers in the bleached region and the scan speed at which the images are acquired. For example, the typical time required to collect a 512×512 image at scan speed of 9 with no line averaging in the Zeiss LSM 510 is ~1 s. For a 70 s recovery, a reasonable sample rate is 75 images at a rate of 1 image/s. A time delay can be used to increase the interval between images to

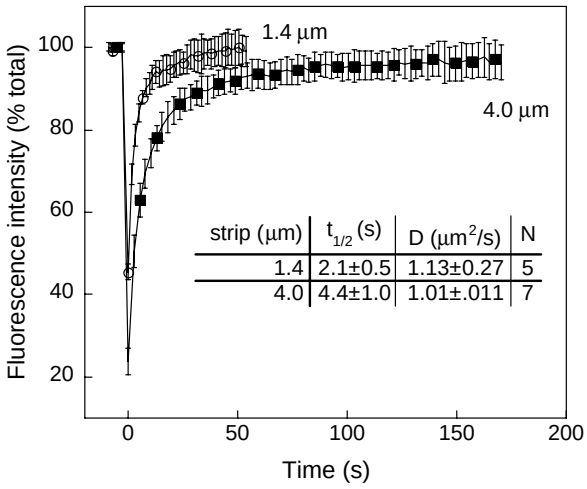

Fig. 5. Kinetics of fluorescence recovery depend on the size of the bleach region for a diffusive process as measured by FRAP. Cells expressing GFP-KRas were bleached using strips either 1.4 wide (circles) or 4-µm wide (squares). The half time for recovery is faster for the smaller strip. Nevertheless, quantitative analysis indicates that the apparent D values are similar for each size box, indicating that the protein is recovering from lateral diffusion. Reproduced from Fig. 3 from *The Journal of Cell Biology, 2004, vol. 165, pp. 735–746* by copyright permission of The Rockefeller University Press.

minimize overall photobleaching during the recovery phase.

3.3.2. Data collection

1. Data are collected using the parameters defined empirically above. Prebleach images are also needed to document initial intensity. We recommend acquiring a minimum of three prebleach images to assess noise and possible bleaching artifacts before the high intensity laser pulse.
2. Generally, at least seven data curves from a particular set of experimental conditions are collected for a given day. Typically, not all the data collected will be usable (see below for examples of typical experimental artifacts).

3.3.3. Confocal FRAP data analysis

(1) *Quantitate the fluorescence intensities.* Once the setup is complete and a series of images is acquired, the intensity values must be documented. For the Zeiss 510 LSM, this is accomplished by selecting the ROI command in the image window. Regions of interest are drawn around the bleached area, the whole cell, and a region outside of the cell for a background value (Fig. 4). To simplify data analysis, consistent order of ROI selection is recommended. Save these data as text files (the default using the Zeiss 510 LSM software) for easy importation into a graphing program for data analysis. The raw data are plotted using a graphing program such as KaleidaGraph. The data are assessed for drifting of the focal plane or bleaching of the sample during low intensity illumination (Figs. 4 and 6).

(2) *Normalize the data.* In order to directly compare recovery curves for different treatments, it is convenient to normalize the data to correct for variations in protein expression levels, background fluorescence F_{bkgd}, and loss of fluorescence during the bleach:

$$F(t)_{\mathrm{norm}} = 100 \times \frac{(F(t)_{\mathrm{ROI}} - F_{\mathrm{bkgd}})}{(F(t)_{\mathrm{cell}} - F_{\mathrm{bkgd}})} \frac{(F_{\mathrm{i\_cell}} - F_{\mathrm{bkgd}})}{(F_{\mathrm{i\_ROI}} - F_{\mathrm{bkgd}})}. \quad (1)$$

Here, the bleached ROI intensity is divided by the whole cell intensity for each time point $F(t)$ to correct for the loss of fluorescence during the bleach. This correction is important when the bleach area is large, because loss a significant fraction of fluorescent material will prevent the recovery from reaching 100% of the prebleach intensity. The data are normalized to the prebleach intensity (F_{i}) and multiplied by 100 to yield a percentage of initial fluorescence. The resulting normalized data then can be averaged for different cells and the associated standard error or standard deviation calculated (Figs. 5, 7, and 8). Also note that in comparing normalized recovery curves, the first time point after the bleach should be set to $t = 0$. This is an approximation since the time required to bleach may be significant depending on the number of bleach iterations. In such a case, further corrections can be made (see, for example [19]).

(3) *Calculate the mobile fraction.* M_{f} is defined as the fraction of molecules that recover during the time course of the experiment. This parameter is sometimes reported as % mobile, in which case the data are multiplied by 100. M_{f} can be calculated from data obtained from the normalized recovery curves (Eq. (1)) as

$$M_{\mathrm{f}} = (F_{\infty} - F_0)/(F_{\mathrm{i}} - F_0), \quad (2)$$

where F_{∞}, F_0, and F_{i} are the normalized fluorescence intensities at the asymptote, immediately following the bleach, and prior to the bleach, respectively (Fig. 1). Note that it is important to include the correction for loss of fluorescence in the bleach area in Eq. (1) in confocal FRAP experiments if the bleach area causes a loss of more than 5% of the available fluorescence. Failure to do so may lead to an underestimate of the true M_{f}.

(4) *Calculate the diffusion coefficient.* The choice of method for calculation of diffusion coefficients depends on the bleach region geometry and type of data collected. Spot photobleaches are classically described by the theory of Axelrod et al. [42]. Here, we outline several examples of approaches that are useful for analysis of confocal FRAP data.

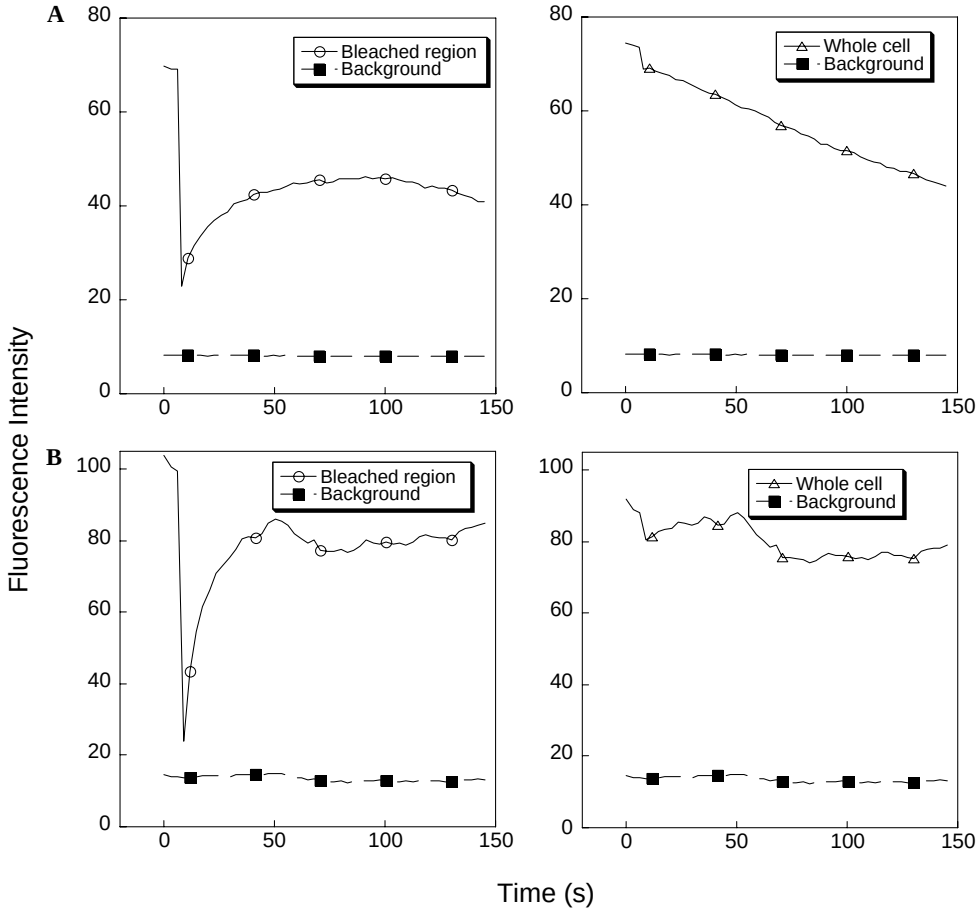

Fig. 6. Example of photobleaching and drifting of the focal plane in a confocal FRAP experiment. Inspection of raw data for both the bleached region (left) and whole cell (right) allows for assessment of technical problems during the experiment. Experiments should be designed to avoid these problems, and curves such as these should not be included in data analysis. (A) Example of overall photobleaching during image acquisition. This is evident from the loss of fluorescence in the whole cell region (right) as well as the drop in fluorescence at the end of the recovery curve in the bleached region (left). Decreasing the laser intensity used to acquire postbleach images and/or increasing detector gain will decrease this effect. (B) Example of focal plane fluctuations. This can occur in response to air currents and/or changes in room temperature. Equilibrating the stage and objective to the desired temperature prior to an experiment helps to eliminate this problem.

a. A program that simulates diffusion in inhomogeneous media is a useful method for confocal FRAP data analysis. This simulation takes into account cell geometry, allows for arbitrary choice of bleach region, and does not require a complete bleach [43]. The program uses images collected from the actual FRAP experiment to simulate diffusive recovery of fluorescent molecules into the bleach region. It calculates an effective diffusion coefficient based on a comparison of the simulated and experimental recoveries. Although this program allows for choice of arbitrary bleach region geometries, we have found that for ease of data analysis it is convenient to maintain a constant geometry (strip) across experiments [26]. Further details on how to obtain and use this simulation can be found in [19].
b. Diffusion into a strip of width w can be approximated by

$$F(t) = F_{\infty}(1 - (w^2(w^2 + 4\pi Dt)^{-1})^{1/2}). \quad (3)$$

This equation assumes that the bleach is complete and that there is no immobile fraction as well as certain geometric constraints [43,44]. Note, however, that estimates of D_{eff} provided by this equation can be off by ~30% [43].
c. Diffusion into a uniform circular disk (as opposed to a Gaussian intensity profile typically used for a spot photobleach) [42,45] can be described by

$$D = 0.224r^2/t_{\text{d}}. \quad (4)$$

Here, r is the radius of the bleached region and t_{d} is the characteristic diffusion time. An example of this equation applied to confocal FRAP measurements can be found in [46].
d. For some applications, such as measurements of combined diffusion and exchange of a protein on and off a membrane [24], the halftime of recovery

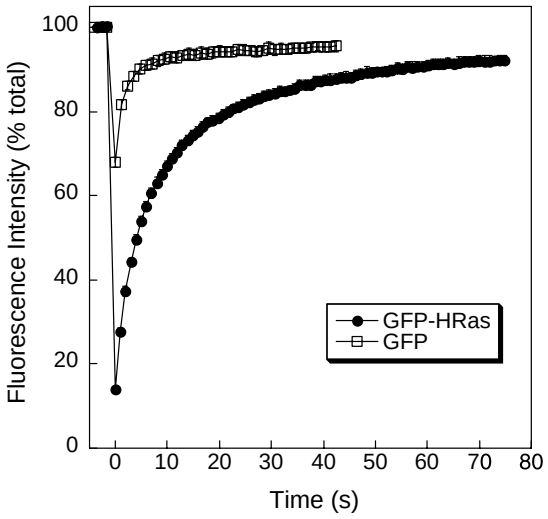

Fig. 7. Diffusion of Ras is significantly slower than a soluble protein. Diffusion of GFP-HRas (circles) is much slower than a soluble protein such as GFP (squares). Because of the fast diffusion of soluble proteins, crucial data generated immediately after recovery are lost before the first time point can be obtained.

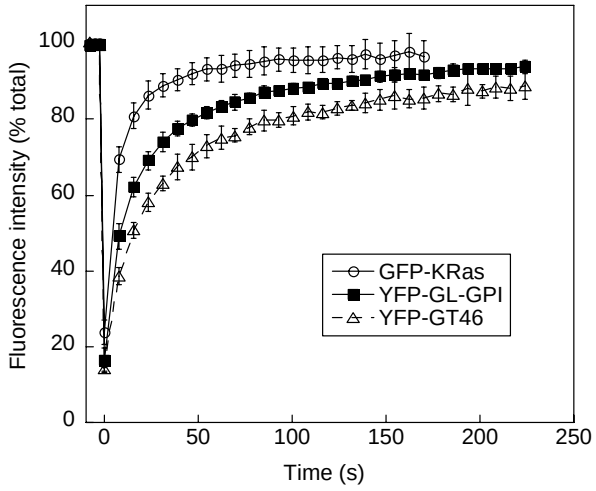

Fig. 8. Diffusion of Ras is fast compared to other plasma membrane proteins. Kinetics of recovery for a transmembrane protein, YFP-GT46 (triangles), a GPI-anchored protein, YFP-GL-GPI (squares), and GFP-KRas (circles) expressed in COS-7 cells. FRAP was performed at 37 °C using a 4-μm-wide bleach box. GFP-KRas with a D of 1.01 ± 0.11 μm^2/s diffuses relatively rapidly when compared to YFP-GL-GPI ($D = 0.47 \pm 0.07$ μm^2/s) and YFP-GT46 ($D = 0.23 \pm 0.02$ μm^2/s). Adapted from Fig. 3 of *The Journal of Cell Biology, 2004, vol. 165, pp. 735–746* by copyright permission of The Rockefeller University Press.

($t_{1/2}$) provides a more appropriate representation of the data than an apparent diffusion coefficient. For a Gaussian spot, the half time of recovery ($t_{1/2}$) can be approximated from

$$F(t) = 100[F_0 + F_\infty(t/t_{1/2})]/[1 + (t/t_{1/2})], \quad (5)$$

where F_0 is the fluorescence intensity immediately after the photobleach and F_∞ is the intensity at the asymptote of the fluorescence recovery after bleaching [47].

3.4. FLIP

1. Follow the FRAP protocol above to determine conditions for imaging.
2. In the EditBleach window using Zeiss 510 LSM software (or equivalent), select "bleach after number of scans," and enter the frequency of bleaching desired. Typically, recovery in the bleach ROI should be allowed to occur as completely as possible before rebleaching.
3. Set the total number of images to collect according to the time it takes to render the cellular compartment of interest dark, remembering to consider the scan time.
4. It is convenient to select fields containing at least two cells for FLIP analysis and perform FLIP on only one of them. The unbleached cell serves as an internal control to monitor the extent of overall photobleaching and/or scattering. To further rule out the possible bleaching artifacts, repeat the FLIP measurements on the fixed cells.
5. FLIP data can be analyzed semi-quantitatively by plotting the loss of fluorescence in the area of interest outside the bleached region [33]. Images from a FLIP experiment can also be analyzed using a simulation of diffusion in inhomogeneous media to yield an effective diffusion coefficient [43].

3.5. Selective photobleaching

1. Follow the FRAP protocol above to determine conditions for imaging.
2. Using the drawing tool, circumscribe a particular region of interest to be bleached. There are no limits to the area selected. As for the case of FRAP, fixed cells are used to determine the conditions required for bleaching.
3. Monitor fluorescent protein movement into the bleached region through time-lapse imaging as for FRAP. Recoveries in the bleached region can be similarly quantitated.
4. Alternatively, selective photobleaching can be used to eliminate background fluorescence in order to better visualize dim structures. For such experiments, it is sometimes necessary to saturate the fluorescence intensity in one region of the cell in order to better visualize structures containing weak fluorescence signals (such as transport intermediates) [34].
5. It is often convenient to perform selective photobleaching on a single cell in a field containing multiple cells in order to provide an internal control for focal plane drift or overall bleaching.

6. Data from selective photobleaching experiments are often usefully combined with kinetic analysis to determine parameter such as the rate of cycling between two compartments (and corresponding residence times within each compartment) or the rate of protein dissociation from membranes [34,48].

4. General considerations for live cell imaging and photobleaching approaches

1. The use of monomeric forms of GFP has been shown to be important for some applications such as fluorescence resonance energy transfer measurements of membrane proteins [49]. Hancock and colleagues [8] have argued that clustering of GFP-Ras detected by electron microscopy is not induced by dimerization of GFP. We have found that the diffusional properties of GFP-tagged versus mGFP-tagged transmembrane and GPI-anchored proteins are similar [26]. Whether monomeric GFP is required for other applications should be tested on a case-by-case basis.
2. In confocal-based photobleaching experiments, the temporal resolution is limited by the time required to collect an image. This can become problematic for measurements of soluble protein diffusion, which is much more rapid than for membrane proteins (Fig. 7). Since the diffusion of Ras is very rapid for a membrane protein ($\sim$1 $\mu m^2/s$) (Fig. 8), it is essential to monitor recoveries as quickly as possible to obtain the most accurate data.
3. Take into account that with more bleach iterations, there is a longer delay before the first postbleach image is acquired. If the protein diffusion is fast, significant recovery may occur during the photobleach episode. Therefore, using the minimum number of iterations needed to bleach the sample is highly recommended.
4. A high NA objective is necessary for maximum signal detection. This allows the laser transmission to be reduced in order to minimize photobleaching when collecting consecutive images.
5. For better quality images, a slower scan speed or line averaging may be necessary. These considerations may also be relevant for dim cells.
6. Recovery times may vary depending on treatments to the cell and the temperature at which the images are collected. For example, D for many proteins increases approximately twofold when the temperature is increased from 25 to 37 °C [26].

5. Applications

5.1. Exchange of Ras on and off membranes

Ras is synthesized as a soluble protein and undergoes a series of posttranslational processing events including farnesylation, proteolysis, and carboxylmethylation which enable it to bind cell membranes (reviewed in [3,50]). Stable membrane binding of Ras additionally requires a second membrane targeting signal consisting of palmitoylation for HRas and NRas or a polybasic domain for KRas [51,52]. Binding of Ras to cell membranes has traditionally been studied by biochemical fractionation of soluble and membrane fractions. Imaging studies of GFP-tagged Ras in living cells offer a new approach to evaluate this question, and importantly can also be used to make measurements at different intracellular sites as well.

For FRAP recoveries that occur solely by lateral diffusion, the characteristic recovery time is proportional to the area illuminated by the laser beam, whereas if dynamic exchange occurs, the recovery also reflects the chemical relaxation time, which is a constant regardless of membrane area and thus beam size [12]. Thus, by testing how the characteristic recovery time varies with spot size, one can test if recovery is purely diffusive, a combination of diffusion and exchange, or purely due to exchange. Using these criteria, the recovery of constitutively active GFP-KRas, GFP-KRas and GFP-HRas are all consistent with lateral diffusion [12,25,26]. In contrast, we find that ER and Golgi-localized Ras mutants appear to undergo significant exchange between a membrane bound and soluble pool [53]. Recent evidence also indicates that the membrane anchor of HRas is not sufficient to mediate stable binding to the plasma membrane [24]. Instead, the membrane anchor, the hypervariable linker domain, and the N-terminal catalytic domain all help determine the strength of HRas binding to the plasma membrane as well as determine their microdomain localization [24]. The two palmitoylation sites of HRas each contribute differently to its plasma membrane binding as well [54]. These observations reveal unexpected complexity in the manner by which the membrane binding of lipid-modified proteins such as Ras is regulated.

5.2. Membrane microdomains and compartmentalization of Ras signaling at the cell surface

A combination of functional, biochemical, and morphological evidence suggests HRas and KRas reside in and signal from distinct classes of membrane microdomains on the inner leaflet of the plasma membrane (reviewed in [4,5,55]). In this model, HRas associates with both cholesterol-dependent (lipid rafts/caveolae) and cholesterol-insensitive domains, but shifts primarily to non-raft domains upon GTP binding. In contrast, KRas resides almost exclusively in non-raft disordered membrane in both its GTP and GDP-bound forms. FRAP experiments of GFP-tagged Ras in living cells have provided further support for this model [12]. In particular, GFP-HRas but not GFP-KRas diffusion in-

creased in response to cholesterol depletion, suggesting its diffusion is constrained by cholesterol-sensitive domains. The diffusion of constitutively active GFP-HRas and GFP-KRas, but not GFP-HRas increased with protein expression levels in a saturable manner, implying that they are confined by a yet undefined domain outside of lipid rafts [12]. Very recently, a similar approach has been used to identify signals within HRas that contribute to its targeting to cholesterol-sensitive domains [24].

The diffusional mobility of GFP-Ras offers additional insights into the nature of its microenvironment. For example, the observation that both GFP-HRas and GFP-KRas diffuse rapidly and exhibit high M_f [12,26] implies that either the association of Ras with these domains is quite dynamic or that the domains themselves are highly mobile. In fact, the diffusion of Ras is lipid-like in the sense that it is sensitive to the viscosity of the plasma membrane [56]. Since the diffusion of GPI-anchored proteins and transmembrane proteins is significantly slower than that of Ras (Fig. 8), it is unlikely that microdomains on the inner leaflet are constitutively linked to domains on the outer leaflet [26]. The diffusional mobility of Ras has also been examined at the level of individual molecules. Recent single molecule tracking studies of GFP appended with the HRas membrane targeting show that 30–40% of molecules are confined in cholesterol-independent domains 200 nm in size [57,58]. Studies of single molecules of YFP-tagged HRas and KRas indicate that the protein becomes strongly immobilized upon activation, perhaps due to the formation of large signaling complexes that are trapped by actin-based corrals [58]. Taken together, these data suggest that Ras dynamically samples a number of membrane microenvironments, that membrane domains on the inner and outer leaflet differ significantly, and that Ras activation may itself affect the ability of the protein to freely diffuse across the cell surface.

Microdomains are not the only mechanism involved in compartmentalization of Ras signaling at the cell surface. In a study utilizing a FRET sensor of Ras activation consisting of YFP-tagged HRas linked to a CFP-tagged Ras binding domain of Raf expressed in PC12 cells, localization of activated Ras to extending neurites was observed. FRAP measurements showed that there is rapid turnover of activated Ras at the neurites, indicating this localization is not due to retention of activated Ras but rather is a consequence of elevated rate of GTP/GDP exchange and low GTPase activity in that subcellular region [59].

5.3. Ras trafficking and intracellular Ras signaling

The finding that the processing and trafficking of newly synthesized Ras to the cell surface involves the secretory pathway raised the possibility that Ras can signal from endomembranes such as the endoplasmic reticulum and Golgi complex (reviewed in [2]). GFP-HRas and GFP-NRas (but not GFP-KRas) localize to the Golgi and this pool of Ras can actively signal [11,60]. Recent studies using selectively photobleaching the Golgi of GFP-H- or NRas have elucidated a novel mechanism for actively maintaining the Golgi pool of Ras [53,61]. This pathway involves a cycle of deacylation and subsequent re-acylation of the protein, allowing it to traffic to and from the Golgi complex through a combination of vesicular and non-vesicular transport [53,61]. Now that several candidate Ras palmitoyltransferases have been identified [62–65], it will be of interest to test their potential role in regulating these events.

Acknowledgments

This work was funded in part by a New Faculty Development Fund from the Department of Molecular Physiology and Biophysics to A.K.K. Preliminary studies were supported by a NICHD-NIH National Research Council Fellowship to A.K.K. We thank Mark Philips for the gift of the GFP-Ras constructs and for helpful discussions.

References

[1] J. Lippincott-Schwartz, E. Snapp, A. Kenworthy, Nat. Rev. Mol. Cell Biol. 2 (2001) 444–456.
[2] T.G. Bivona, M.R. Philips, Curr. Opin. Cell Biol. 15 (2003) 136–142.
[3] T. Magee, C. Marshall, Cell 98 (1999) 9–12.
[4] J.F. Hancock, Nat. Rev. Mol. Cell Biol. 4 (2003) 373–384.
[5] R.G. Parton, J.F. Hancock, Trends Cell Biol. 14 (2004) 141–147.
[6] I.A. Prior, A. Harding, J. Yan, J. Sluimer, R.G. Parton, J.F. Hancock, Nat. Cell Biol. 3 (2001) 368–375.
[7] I.A. Prior, R.G. Parton, J.F. Hancock, Sci. STKE 2003 (2003) PL9.
[8] I.A. Prior, C. Muncke, R.G. Parton, J.F. Hancock, J. Cell Biol. 160 (2003) 165–170.
[9] S. Roy, R. Luetterforst, A. Harding, A. Apolloni, M. Etheridge, E. Stang, B. Rolls, J.F. Hancock, R.G. Parton, Nat. Cell Biol. 1 (1999) 98–105.
[10] E. Choy, V.K. Chiu, J. Silletti, M. Feoktistov, T. Morimoto, D. Michaelson, I.E. Ivanov, M.R. Philips, Cell 98 (1999) 69–80.
[11] V.K. Chiu, T. Bivona, A. Hach, J.B. Sajous, J. Silletti, H. Wiener, R.L. Johnson 2nd, A.D. Cox, M.R. Philips, Nat. Cell Biol. 4 (2002) 343–350.
[12] H. Niv, O. Gutman, Y. Kloog, Y.I. Henis, J. Cell Biol. 157 (2002) 865–872.
[13] M. Edidin, in: S. Damjanovich, M. Edidin, J. Szollosi, L. Tron (Eds.), Mobility and Proximity in Biological Membranes, CRC Press, Boca Raton, FL, 1994, pp. 109–135.
[14] T.K. Meyvis, S.C. De Smedt, P. Van Oostveldt, J. Demeester, Pharm. Res. 16 (1999) 1153–1162.
[15] A.B. Houtsmuller, W. Vermeulen, Histochem. Cell Biol. 115 (2001) 13–21.
[16] E.A. Reits, J.J. Neefjes, Nat. Cell Biol. 3 (2001) E145–E147.
[17] G. Carrero, D. McDonald, E. Crawford, G. de Vries, M.J. Hendzel, Methods 29 (2003) 14–28.

[18] M. Edidin, Trends Cell Biol. 2 (1992) 376–380.
[19] E.L. Snapp, N. Altan, J. Lippincott-Schwartz, in: J.S. Bonifacino, M. Dasso, J.B. Harford, J. Lippincott-Schwartz, K. Yamada (Eds.), Current Protocols in Cell Biology, vol. 3, Wiley, NY, 2003, pp. 21.1–21.1.24.
[20] P. Schwille, J. Korlach, W.W. Webb, Cytometry 36 (1999) 176–182.
[21] K. Ritchie, A. Kusumi, Methods Enzymol. 360 (2003) 618–634.
[22] G.H. Patterson, J. Lippincott-Schwartz, Science 297 (2002) 1873–1877.
[23] G.H. Patterson, J. Lippincott-Schwartz, Methods 32 (2004) 445–450.
[24] B. Rotblat, I.A. Prior, C. Muncke, R.G. Parton, Y. Kloog, Y.I. Henis, J.F. Hancock, Mol. Cell. Biol. 24 (2004) 6799–6810.
[25] H. Niv, O. Gutman, Y.I. Henis, Y. Kloog, J. Biol. Chem. 274 (1999) 1606–1613.
[26] A.K. Kenworthy, B.J. Nichols, C.L. Remmert, G.M. Hendrix, M. Kumar, J. Zimmerberg, J. Lippincott-Schwartz, J. Cell Biol. 165 (2004) 735–746.
[27] S. Nehls, E.L. Snapp, N.B. Cole, K.J. Zaal, A.K. Kenworthy, T.H. Roberts, J. Ellenberg, J.F. Presley, E. Siggia, J. Lippincott-Schwartz, Nat. Cell Biol. 2 (2000) 288–295.
[28] P. Thomsen, K. Roepstorff, M. Stahlhut, B. van Deurs, Mol. Biol. Cell 13 (2002) 238–250.
[29] T. Shimi, T. Koujin, M. Segura-Totten, K.L. Wilson, T. Haraguchi, Y. Hiraoka, J. Struct. Biol. 147 (2004) 31–41.
[30] A. Birbach, S.T. Bailey, S. Ghosh, J.A. Schmid, J. Cell Sci. 117 (2004) 3615–3624.
[31] Y. Chai, J. Shao, V.M. Miller, A. Williams, H.L. Paulson, Proc. Natl. Acad. Sci. USA 99 (2002) 9310–9315.
[32] S.A. Endow, D.W. Piston, in: M. Chalfie, S. Kain (Eds.), Green Fluorescent Protein: Properties, Applications, and Protocols, Wiley-Liss, New York, 1998, pp. 320–356.
[33] N.B. Cole, C.L. Smith, N. Sciaky, M. Terasaki, M. Edidin, J. Lippincott-Schwartz, Science 273 (1996) 797–801.
[34] B.J. Nichols, A.K. Kenworthy, R.S. Polishchuk, R. Lodge, T.H. Roberts, K. Hirschberg, R.D. Phair, J. Lippincott-Schwartz, J. Cell Biol. 153 (2001) 529–541.
[35] T.H. Ward, R.S. Polishchuk, S. Caplan, K. Hirschberg, J. Lippincott-Schwartz, J. Cell Biol. 155 (2001) 557–570.
[36] A. Apolloni, I.A. Prior, M. Lindsay, R.G. Parton, J.F. Hancock, Mol. Cell. Biol. 20 (2000) 2475–2487.
[37] X. Jiang, A. Sorkin, Mol. Biol. Cell 13 (2002) 1522–1535.
[38] M.A. Rizzo, C.A. Kraft, S.C. Watkins, E.S. Levitan, G. Romero, J. Biol. Chem. 276 (2001) 34928–34933.
[39] S. Roy, B. Wyse, J.F. Hancock, Mol. Cell. Biol. 22 (2002) 5128–5140.
[40] J.A. Thissen, J.M. Gross, K. Subramanian, T. Meyer, P.J. Casey, J. Biol. Chem. 272 (1997) 30362–30370.
[41] K. Hirschberg, R.D. Phair, J. Lippincott-Schwartz, Methods Enzymol. 327 (2000) 69–89.
[42] D. Axelrod, D.E. Koppel, J. Schlessinger, E. Elson, W.W. Webb, Biophys. J. 16 (1976) 1055–1069.
[43] E.D. Siggia, J. Lippincott-Schwartz, S. Bekiranov, Biophys. J. 79 (2000) 1761–1770.
[44] J. Ellenberg, E.D. Siggia, J.E. Moreira, C.L. Smith, J.F. Presley, H.J. Worman, J. Lippincott-Schwartz, J. Cell Biol. 138 (1997) 1193–1206.
[45] D.M. Soumpasis, Biophys. J. 41 (1983) 95–97.
[46] C.L. Adams, Y.-T. Chen, S.J. Smith, W.J. Nelson, J. Cell Biol. 142 (1998) 1105–1119.
[47] T.J. Feder, I. Brust-Mascher, J.P. Slattery, B. Baird, W.W. Webb, Biophys. J. 70 (1996) 2767–2773.
[48] J.F. Presley, T.H. Ward, A.C. Pfeifer, E.D. Siggia, R.D. Phair, J. Lippincott-Schwartz, Nature 417 (2002) 187–193.
[49] D.A. Zacharias, J.D. Violin, A.C. Newton, R.Y. Tsien, Science 296 (2002) 913–916.
[50] J.R. Silvius, J. Membr. Biol. 190 (2002) 83–92.
[51] J.F. Hancock, K. Cadwallader, C.J. Marshall, EMBO J. 10 (1991) 641–646.
[52] J.F. Hancock, H. Paterson, C.J. Marshall, Cell 63 (1990) 133–139.
[53] J.S. Goodwin, K.R. Drake, C. Rogers, L. Wright, J. Lippincott-Schwartz, M.R. Philips, A.K. Kenworthy, J. Cell Biol. 170 (2005) 261–272.
[54] S. Roy, S. Plowman, B. Rotblat, I.A. Prior, C. Muncke, S. Grainger, R.G. Parton, Y.I. Henis, Y. Kloog, J.F. Hancock, Mol. Cell. Biol. 25 (2005) 6722–6733.
[55] I.A. Prior, J.F. Hancock, J. Cell Sci. 114 (2001) 1603–1608.
[56] J.S. Goodwin, K.R. Drake, C.L. Remmert, A.K. Kenworthy, Biophys. J. 89 (2005) 1398–1410.
[57] P.H. Lommerse, G.A. Blab, L. Cognet, G.S. Harms, B.E. Snaar-Jagalska, H.P. Spaink, T. Schmidt, Biophys. J. 86 (2004) 609–616.
[58] H. Murakoshi, R. Iino, T. Kobayashi, T. Fujiwara, C. Ohshima, A. Yoshimura, A. Kusumi, Proc. Natl. Acad. Sci. USA 101 (2004) 7317–7322.
[59] N. Mochizuki, S. Yamashita, K. Kurokawa, Y. Ohba, T. Nagai, A. Miyawaki, M. Matsuda, Nature 411 (2001) 1065–1068.
[60] T.G. Bivona, I. Perez De Castro, I.M. Ahearn, T.M. Grana, V.K. Chiu, P.J. Lockyer, P.J. Cullen, A. Pellicer, A.D. Cox, M.R. Philips, Nature 424 (2003) 694–698.
[61] O. Rocks, A. Peyker, M. Kahms, P.J. Verveer, C. Koerner, M. Lumbierres, J. Kuhlmann, H. Waldmann, A. Wittinghofer, P.I. Bastiaens, Science 307 (2005) 1746–1752.
[62] J.E. Smotrys, M.E. Linder, Annu. Rev. Biochem. 73 (2004) 559–587.
[63] K. Huang, A. Yanai, R. Kang, P. Arstikaitis, R.R. Singaraja, M. Metzler, A. Mullard, B. Haigh, C. Gauthier-Campbell, C.A. Gutekunst, M.R. Hayden, A. El-Husseini, Neuron 44 (2004) 977–986.
[64] C.E. Ducker, E.M. Stettler, K.J. French, J.J. Upson, C.D. Smith, Oncogene 23 (2004) 9230–9237.
[65] J.T. Swarthout, S. Lobo, L. Farh, M.R. Croke, W.K. Greentree, R.J. Deschenes, M.E. Linder, J. Biol. Chem. (2005).